International Journal of Progressive Sciences and Technologies (IJPSAT)
ISSN: 2509-0119.

Vol. 38 No. 1 April 2023, pp. 566-575

Optimization Of The Vertical Axis Wind Turbine For Localization In Low Wind Speed Areas

Joweria Totokoja[1], Samson Rwahwire (PhD)[2], Joseph Lwanyaga Ddumba (PhD)[3], Ayub Nabende[1] , Moses Nagulama[1]

[1]Department of Mathematics, Faculty of Science and Education, Busitema University.
[2]Department of Polymer, Textile & Industrial Engineering, Faculty of Engineering, Busitema University.
[3]Department of Mining & Water Resource Engineering, Faculty of Engineering, Busitema University.

Abstract – The vertical axis wind turbines (VAWTs) have proved to show how they are well suited for the urban landscape in production of renewable energy. Thus, the major objective of this study was to develop an optimal model for the vertical axis wind turbine using Computational Fluid Dynamics (CFD). VAWT blades are designed in such a way that they exhibit good aerodynamic performance throughout an entire rotation at various angles of attack they experience leading to optimal performance. In this study, an average unsteady wind flow speed of 10 ms^{-1} was considered to flow towards the VAWT at angles of attack ranging from 0^o to 18^o. The NACA0012 airfoil blade was used to study the aerodynamic factors on the VAWT and optimize its performance using the CFD software ANSYS Fluent 7.2. A CFD analysis method was used to evaluate both unsteady wind inflow performance and the flow hydraulics that affects the performance of a VAWT. Mathematical model formulations and numerical simulations using Reynolds Averaged Navier-Stokes (RANS) are employed. The k-ω turbulence model was found to perform well for unsteady wind flow simulations for optimal performance of the VAWT. The numerical simulations of velocity and pressure contours at different angles of attack were analysed in consideration of the lift and drag forces. The NACA0012 airfoil blade was found to perform optimally at angles of attack in the range $0^o \leq \alpha \leq 16^o$.

Keywords – Vertical Axis Wind Turbine, Computational Fluid Dynamics, Model Equations, angle of attack.

I. INTRODUCTION

Wind is a source of renewable energy which is clean, environment friendly, cost effective and contributes less or no greenhouse gases throughout its operational cycle (Ralon et al., 2017). This makes wind energy to be a viable renewable energy resource towards a balanced future for the ever increasing population worldwide. According to Twaha et al. (2016), several studies on the speed of wind across the regions of Uganda have shown that there sensible winds to generate power energy having a mean speeds at several altitudes from 1.8 ms^{-1} to about 4 ms^{-1}. However, there are limited studies on wind energy utilization as much attention is put to solar energy as the alternative to hydro-power.

Vertical axis wind turbines (VAWTs) are considered to be more promising energy conversion devices due to a variety of brand new methods that can put forward their performance and efficiency (Wang and Zhuang, 2017). Unlike the horizontal axis wind turbine (HAWT) where the blades only operate at a single angle of attack throughout an entire rotation, VAWT blades are designed in such a way that they exhibit good aerodynamic performance throughout an entire rotation at the various angles of attack they experience leading to high time averaged torque (McLaren et al., 2012). Additionally, VAWTs have distinct operating features such as; ability to operate under irregular wind flow, slow cut-in speed and low maintenance cost (Hui et al., 2018). Thus, VAWTs can be utilized for urban wind generation due to the slower, more turbulent and multi-directional characteristics of wind in most cities and towns like Tororo municipality.

Corresponding Author: Joweria Totokoja

Numerical Modeling of the VAWT

Computational fluid dynamics (CFD) modeling is able to numerically predict wind turbine performance as it offers a tremendous benefit of being more economical than experimental techniques (Wekesa et al.,2014). CFD is a key contributor in designing, analyzing, monitoring and virtual prototyping of everything involving wind turbine development (Versteeg and Malalasekera, 2007). Chowdhury et al. (2016) conducted a rigorous parametric study on the aerodynamic characteristics of VAWT in tilted condition. The CFD simulations of the VAWT were performed by solving the unsteady RANS equations using CFD open source package OpenFoam. They implied that the power coefficient of the VAWT is directly influenced by upright position of the turbine, especially the tilted angle of the blade configuration. They maintained that tilted condition less than three-degree slope is likely to improve the performance characteristics of the VAWT, however low wind speed conditions where not considered. Therefore, this study sought to create a mathematical model using ANSYS Fluent CFD tool to optimize the performance of the VAWTs in localized low wind speed areas at various angles of attack.

II. METHODOLOGY

The mathematical model formulation and algorithm design was done using CFD analysis and simulations were carried out using the CFD software ANSYS Fluent 17.2.

Mathematical model for the VAWT

The mathematical model formulation of wind flow to the VAWT is comprised of a set of partial differential equations, consisting of the continuity equation, Reynolds Averaged-Navier-Stokes (RANS) equations (Fagbade et al., 2019; Danao, 2014; Versteeg and Malalasekera, 2007). The model equations were solved together with model boundary conditions.

$$\frac{\partial \rho}{\partial t} + \nabla.(\rho U) = 0$$

$$\frac{\partial (\rho U)}{\partial t} + \nabla.(\rho UU) = -\nabla p + \rho g + \nabla.\tau$$

Where U = fluid flow velocity, g = acceleration due to gravity acting of the fluid flow, p = fluid pressure, ρ = fluid density and τ = mean viscous stress tensor characteristically

defined by the fluid type. The components of the mean shear stress tensor τ_{ij}, for i, j taking values 1, 2, 3, ($i \neq j$) are given as;

$$\tau = \tau_{ij} = \mu\left(\frac{\partial U_i}{\partial x_j} + \frac{\partial U_j}{\partial x_i}\right) - \rho \acute{U}_i' \acute{U}_j'$$

Where $\rho \acute{U}_i' \acute{U}_j'$ represents the Reynolds stress term due to turbulent motion. The fluctuating velocity components U_i' , U_j' are further modelled by using the Boussinesq hypothesis (Danao et al., 2014), where Reynolds stress is proportional to the mean velocity gradient as in equation below;

$$\rho \acute{U}_i' \acute{U}_j' = \mu_t\left(\frac{\partial U_i}{\partial x_j} + \frac{\partial U_j}{\partial x_i}\right) - \rho\frac{2}{3}k\delta_{ij}$$

Where δ_{ij} = Kronecker delta defined as;

$$\delta_{ij} = \begin{cases} 1 if i = j \\ 0 if i \neq j \end{cases}$$

Also μ_t is turbulent viscosity given by $\mu_t = C_\mu \rho \frac{k^2}{\varepsilon}$

Turbulent viscosity depends on the turbulence kinetic energy k and its dissipation rate **ε** and C_μ, is the turbulent model constant equal to 0.09 (ANSYS, 2016; Danao et al., 2014). According to Fagbade et al. (2019), to model the turbulence flow of the fluid toward VAWT, the distinct way of describing the turbulent length scale is via the k-ω model as compared to the k- **ε** turbulence model. Therefore, this considered the study k- ω turbulence model to describe the wind flow towards the Vertical axis wind turbine.

The standard k- ω a two-equation model, one for k and the other for ω was formulated by Wilcox (2008) and employs the turbulent frequency $\omega = \frac{\varepsilon}{k}$ so that the length scale of the model becomes.

$$l = \frac{\sqrt{k}}{\omega}$$

Using this length scale, the turbulent viscosity of the model is given as

$$\nu_t = \frac{k}{\omega}$$

The transport equations for turbulent kinetic energy k, and turbulence frequency ω are expressed as

$$\frac{\partial \rho k}{\partial t} + \nabla.(\rho k U) = \nabla.\left(\mu + \frac{\mu_t}{\sigma_{k1}}\nabla k\right) + P_k - \beta \rho k \omega$$

$$\frac{\partial \rho \omega}{\partial t} + \nabla.(\rho \omega U) = \nabla.\left(\mu + \frac{\mu_t}{\sigma_{\omega 1}}\nabla \omega\right) + P_\omega - \beta^1 \rho \omega^2$$

Where P_k and P_k represent the production terms for the turbulent kinetic energy k and w respectively. The model constants σ_{k1}, $\sigma_{\omega 1}$, β and β^1 are given with values 0.85, 0.65, 0.09, 0.075 (ANSYS, 2016; Menter, 1994).

The model equations were numerically solved using the pressure based solver obtained in ANSYS Fluent 17.2 software to determine the fluid flow variable fields for velocity U, pressure p, at different angles of attack in the flow domain of the VAWT.

III. Results and Discussions

The simulation results of the air (wind) flow through the VAWT airfoil blades are completed with the help of the ANSY Fluent17.2 package. CFD is used to predict the air flow pattern and the power output of the VAWT. The results are presented in both graphical and tabular forms to illustrate possible trends of the aerodynamic characteristics. Numerical simulations for the flow around VAWT more so around the NACA 0012 airfoil blades for various angles of attack (a) are presented. The values for optimal performance parameters of the VAWT, the velocity and pressure contours or fields around the VAWT airfoils are presented and the plots of lift and drag coefficient as obtained during the simulations at different angles of attack.

VAWT Optimisation parameters

For the optimal model of the VAWT the following performance parameters, that is, Tip speed ratio, TSR (λ) which is an important factor in wind turbine design, VAWT solidity (σ) and the instantaneous wind power (P_w) were determined; The expression for TSR (λ) is expressed as

$$\lambda = \frac{Velocityatthebladetip}{Incomingwindspeed} = \frac{R \times \omega}{U_\infty}$$

Where R = distance from the center to the mid-point of airfoil or blade (rotating radius of VAWT) which was taken as 0.35m. The angular velocity (ω) was set to 130 rad/s and incoming wind speed was 10 m/s. Thus, TSR (λ) is 4.55.

The solidity was obtained from Equation below, where number of blades (N) was three (3), blade chord length (l_c) as 0.04m and radius of the rotor (R) as 0.35m. These values are substituted as;

$$\sigma = \frac{N l_c}{R} = 0{:}3429$$

The instantaneous wind power is expressed using expression;

$$P_w = \frac{1}{2}\rho A_r U_\infty^3$$

The swept area $A_r = 2Rl$, where l is the blade length (0.6m), ρ is the air density (1.225 kgm^{-3}) and U_∞= 10m/s as the free stream wind speed. Substituting the values, P_W = 257.25W

Velocity flow contours.

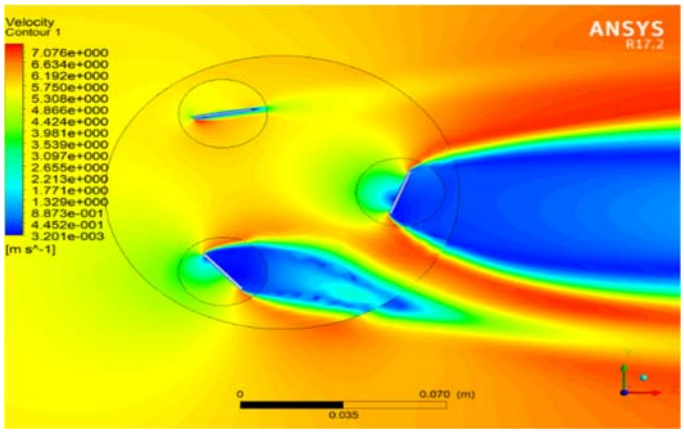

Figure 1: Velocity field around the VAWT and blades at α = 0º

In Figure 1, At 0º angle of attack the free stream wind flow at 10 m/s towards the rotating VAWT tends to fluctuate around the airfoil blades. The average maximum flow velocity of about 7.1 m/s is created at the tips of the blades. When the blade tends orient perpendicular to the flow, a huge recirculation bubble is made, more so around blade two and three. Maximum velocity is created at the lower surface of blade one and Also since blade one is almost aligned with the flow, the flow does not propagate much (is less intense). There is steady rise in velocity profile near the section of the blade surfaces due to high turbulent flow formation within the rotating region. The increment in the velocity distributions impacts the aerodynamic forces acting along the lateral section of the turbine blades and constitutes a greater pressure difference that boost force generation on the blades.

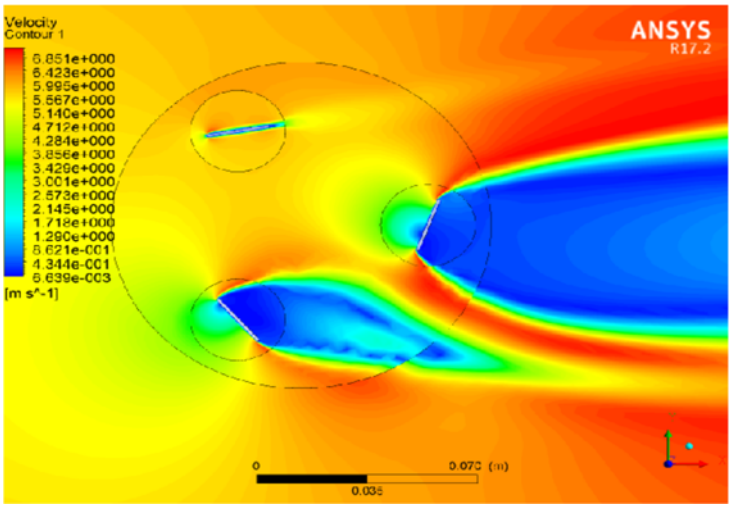

Figure 2: Velocity contours around airfoil blades at α = 4º

Figure 2, shows that at 4º angle of attack, there is high orientation of the blades for the rotating

turbine. Since the blade two and three tend to orient perpendicular to the flow, the velocity is low on the opposite side to the flow. However, the flow velocity is high towards the opposite blade. Maximum average speed of 7.38 m/s is created during the flow towards the blades as compared to flow at 0º angle of attack. This average flow velocity increase leads to an increase of lift force, however rise in drag is small compared to rise in lift force.

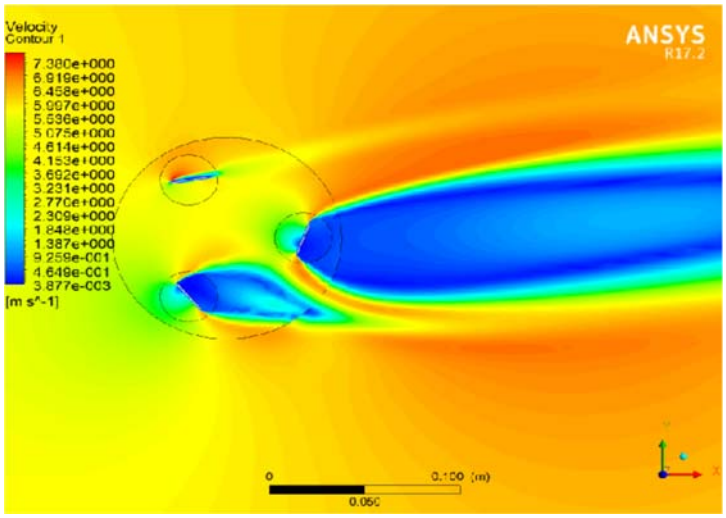

Figure 3: Velocity contours around airfoil blades at α = 8º.

As, α (angle of attack), is increased to 8 degrees as shown in Figures 3, the stagnation point moves towards the trailing edge of the blades two and three. At this angle of attack, there is decrease in the flow velocity between blade two and three. The huge re-circulation bubble of low flow speed made between blades negatively affects the other blade's orientation. The low velocity stream at the leading edge is about 1.327 m/s and flow tends to separate at the trailing edge between the blades.

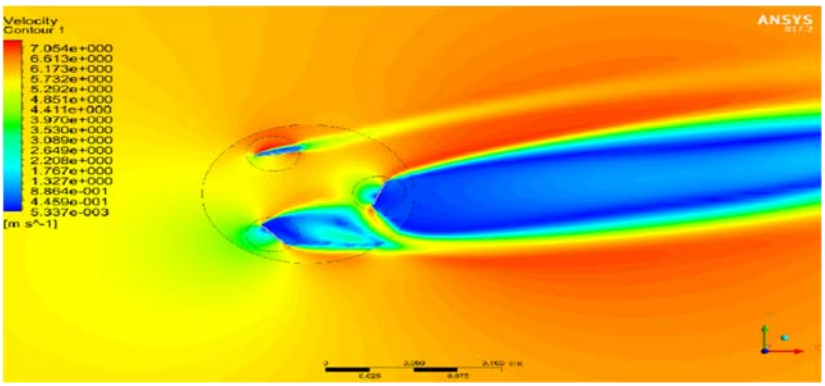

Figure 4: Velocity fields around the airfoil blades at α = 12º.

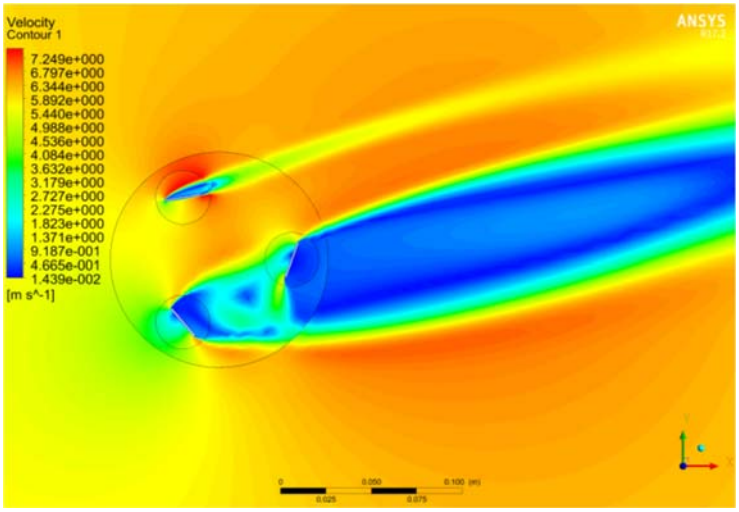

Figure 5: Velocity contours around the airfoil at a = 16º.

Figures 4 and Figure 5, show that increase of a from 0º to 16º results in increased flow speed on the upper surface compared to lower surface of the airfoil blade one. Also as the angle of attack is increased, the stagnation point is created between blade two and three. This shows that for the spinning turbine, increase in the angle of attack affects the orientation of the blades hence optimal performance of the vertical axis wind turbine.

Pressure contours

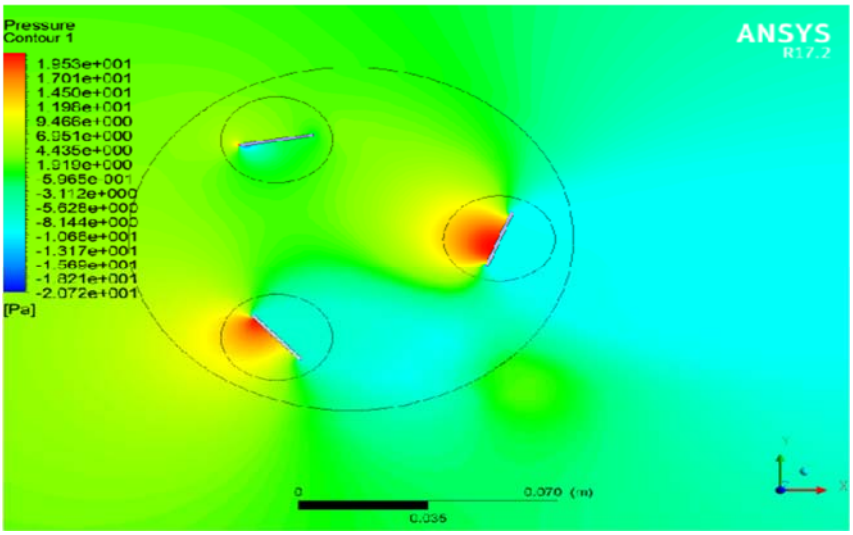

Figure 6: Pressure contours around VAWT and airfoil blades at α =0º

Figure 6 show that at α = 0º, pressure on the blades reach maximum values of about 19.53 Pa more so on blade three. There is highly non-uniform pressure distributions on the blade surfaces in rotating domain, and stationary domain of the VAWT at incoming wind speed of 10 m/s. Greater difference of pressure distribution is observed on airfoil surfaces, where turbulent kinetic energy transfer occurs, leading to more power generation. High pressure regions are noticed within the rotating domain and on the surfaces of the blades, whereas moderate pressure profiles are observed at the rear end with significant reduction within the wind turbine wake.

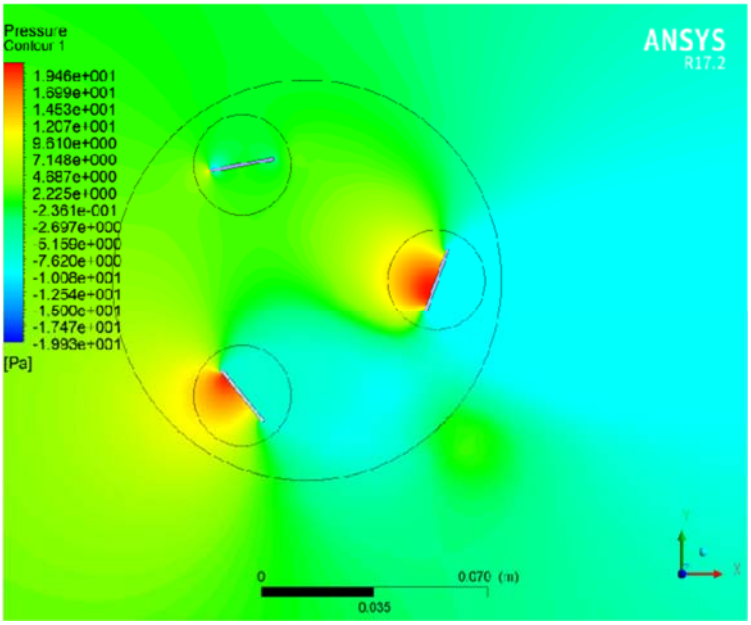

Figure 7: Pressure fields around airfoil blades at α = 4º

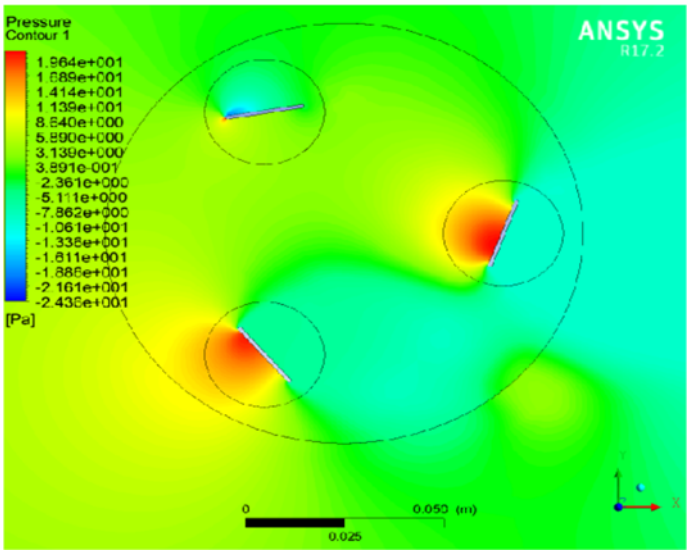

Figure 8: Pressure fields around the VAWT blades at α = 8º

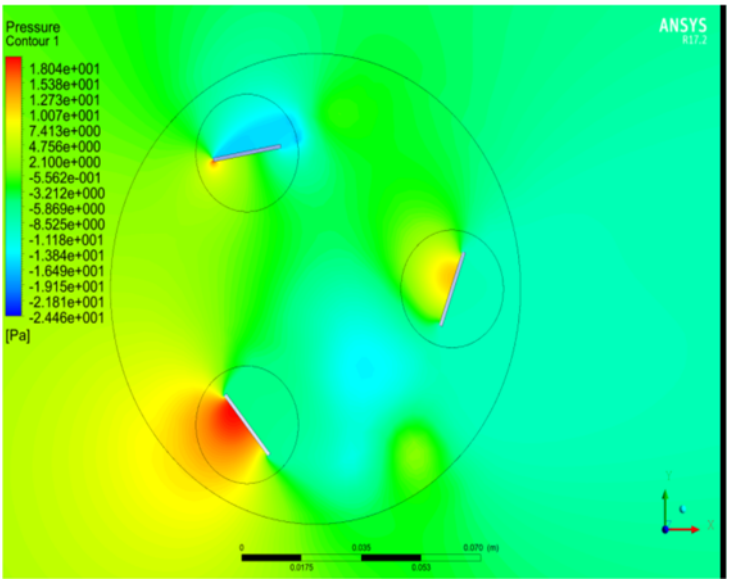

Figure 9: The pressure contours around the blades at a = 16º

As shown in Figure 7 to Figure 9, It is observed that there is gradual increase in the pressure distributions along the blade surfaces from the upstream side of the rotating domain to the downstream side. Also, its observed that the lower side of the blade camber has lower pressure distributions compared to the upper side of the camber. The observed pressure difference is due primarily to the three-dimensional rotatory effect, dynamic flow separation on the blades, and the angle of attack of the blades surfaces to the incoming free-stream wind velocity. The positive and negative pressure distribution regions and their difference accounts for the turbine rotation. The pressure difference between the lower and upper part of the airfoil results in lift force, caused by increasing the angle of attack from 0º to 16º. This results in pressure increment on the other surface of the airfoil, hence increment in lift force as the angle of attack increases.

Figure 9, shows that as the angle of attack rises above 12 degrees ($\alpha > 12^o$) to stall point, maximum value attained by the blades is about 18.04 Pa, thus there is reduced pressure on the blades which tends to affect their orientation.

Effect of Lift and Drag forces on the VAWT blade

Figure 10 shows that at angles of attack 0º to about 14º, the lift force increase proportionally with angle of attack. This implies that flow is attached to the airfoil throughout this regime.

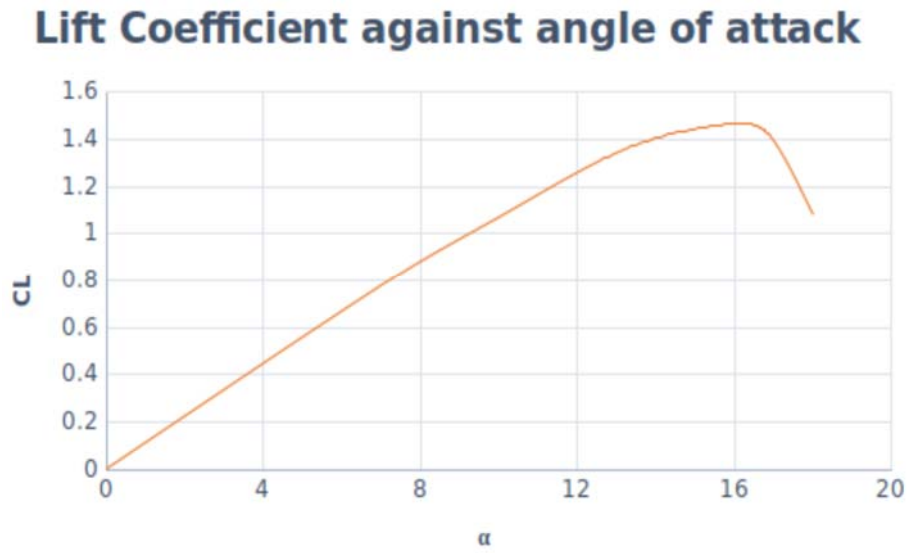

Figure 10: Graph of lift coefficient with angle of attack at inflow speed (U_∞).

At an angle of attack of roughly 15º to 16º, the flow on the upper surface of the airfoil begins to separate and a condition known as stall begin to develop. The lift is maximum of about $C_l = 1.45$ at an angle of attack $\alpha = 16°$, there after lift reduces. Hence the stall angle tends to be about $16°$.

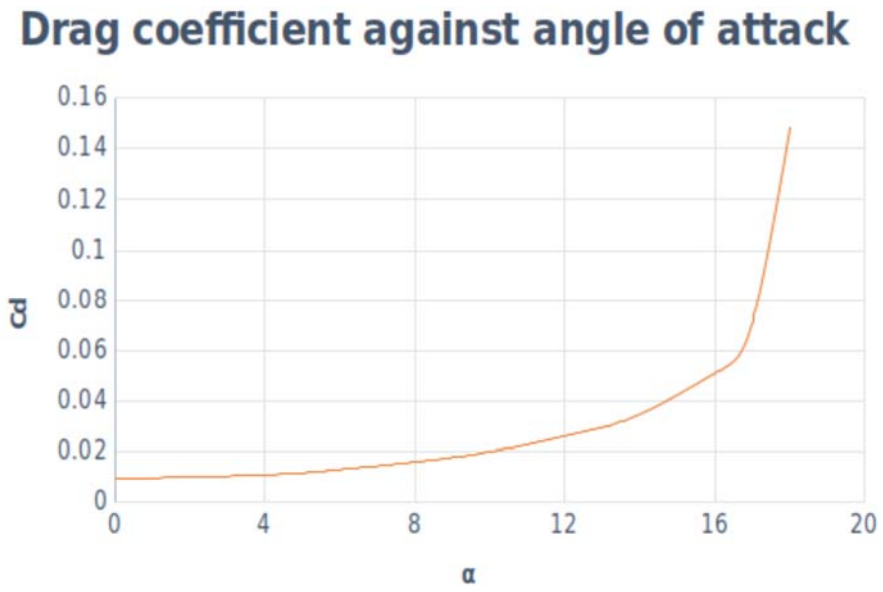

Figure 11: Plot of drag coefficient against angle of attack.

The drag is small for angles of attack from 0º to about 16º as expected and increases at a faster rate with increasing angle of attack as shown in Figure 11. This indicates that greater amount of drag on the VAWT blade results into low lift coefficient.

IV. CONCLUSIONS

The optimal performance of the vertical axis wind turbine (VAWT) depends on its design. The choice of airfoil profile is critical to the VAWT aerodynamics as this dictates the point and time of stall. From an aerodynamic point of view, the NACA0012 blade type are preferred in large scale VAWTs due to increased torque generation as a result of high pressure gradients. Therefore, NACA0012 airfoil is able to optimize the power output when used in the design of the VAWT. This is to the fact that increase in the lift forces is high as compared to the drag forces, which facilitates the increase in the torque on the turbine, thus rotation of the wind turbine.

Numerical simulations show that the airfoil blade of the VAWT is able to perform optimally at angles of attack in the range $0° \leq \alpha \leq 16°0$. Thus the VAWT turbine is able to perform effectively and optimize the power output even at low wind speeds.

Rather than depend on the wind tunnel experiments that can be costly, risky, and easily influenced by the instability and interference in evaluating the performance characteristics of the wind turbine, one can undertake CFD simulations to produce cost-effective wind turbine performance assessment.

REFERENCES

[1] ANSYS, A. (2016). Ansys fluent users guide, 17.2. Canonsburg: ANSYS.

[2] Beri, H., Yao, Y., et al. (2011). Effect of camber airfoil on self-starting of vertical axis wind turbine. Journal of environmental Science and Technology, 4(3):302–312.

[3] Chowdhury, A. M., Akimoto, H., and Hara, Y. (2016). Comparative CFD analysis of vertical axis wind turbine in upright and tilted configuration. Renewable Energy, 85:327–337.

[4] Danao, L. A. (2014). The influence of unsteady wind on the performance and aerodynamics of vertical axis wind turbines. PhD thesis, University of Sheffield.

[5] Danao, L. A., Edwards, J., Eboibi, O., and Howell, R. (2014). A numerical investigation into the influence of unsteady wind on the performance and aerodynamics of a vertical axis wind turbine. Applied Energy, 116:111–124.

[6] Das, A. and Talapatra, P. K. (2016). Modelling and analysis of a mini vertical axis wind turbine. International Journal of Emerging technology and Advanced Engineering, 6(6).

[7] Fagbade, A. I. et al. (2019). Numerical Simulation of the Lux Vertical Axis Wind Turbine. PhD thesis, University of Saskatchewan.

[8] Ferreira, C. S., Bijl, H., Van Bussel, G., and Van Kuik, G. (2007). Simulating dynamic stall in a 2D VAWT: modeling strategy, verification and validation with particle image velocimetry data. In Journal of physics: conference series, volume 75, pages 12–23. Institute of Physics.

[9] Howell, R., Qin, N., Edwards, J., and Durrani, N. (2010). Wind tunnel and numerical study of a small vertical axis wind turbine. Renewable energy, 35(2):412–422.

[10] Hui, I., Cain, B. E., and Dabiri, J. O. (2018). Public receptiveness of vertical axis wind turbines. Energy Policy, 112:258–271.

[11] McLaren, K., Tullis, S., and Ziada, S. (2012). Computational fluid dynamics simulation of the aerodynamics of a high solidity, small-scale vertical axis wind turbine. Wind Energy, 15(3):349–361.

[12] Menter, F. R. (1994). Two-equation eddy-viscosity turbulence models for engineering applications. AIAA journal, 32(8):1598–1605.

[13] Raciti Castelli, M., Ardizzon, G., Battisti, L., Benini, E., and Pavesi, G. (2010). Modeling strategy and numerical validation for a darrieus vertical axis micro-wind turbine. In ASME International Mechanical Engineering Congress and Exposition, volume 44441, pages 409–418.

[14] Rahman, M., Morshed, K. N., Lewis, J., and Fuller, M. (2009). Experimental and numerical investigations on drag and torque characteristics of three-bladed savonius wind turbine. In ASME International Mechanical Engineering Congress and Exposition, volume 43796, pages 85–94.

[15] Ralon, P., Taylor, M., Ilas, A., Diaz-Bone, H., and Kairies, K. (2017). Electricity storage and renewables: Costs and markets to 2030. International Renewable Energy Agency: Abu Dhabi, UAE.

[16] Rezaeiha, A., Kalkman, I., and Blocken, B. (2017). Cfd simulation of a vertical axis wind turbine

[17] operating at a moderate tip speed ratio: guidelines for minimum domain size and azimuthal increment. Renewable energy, 107:373–385.

[18] Saha, U., Thotla, S., and Maity, D. (2008). Optimum design configuration of savonius rotor through wind tunnel experiments. Journal of Wind Engineering and Industrial Aerodynamics, 96(8-9):1359–1375.

[19] Twaha, S., Ramli, M. A., Murphy, P. M., Mukhtiar, M. U., and Nsamba, H. K. (2016). Renewable based distributed generation in Uganda: Resource potential and status of exploitation. Renewable and Sustainable Energy Reviews, 57:786–798.

[20] Versteeg, H. K. and Malalasekera,W. (2007). An introduction to computational fluid dynamics: the finite volume method. Pearson education.

[21] Wang, Z. and Zhuang, M. (2017). Leading-edge serrations for performance improvement on a verticalaxis wind turbine at low tip-speed-ratios. Applied energy, 208:1184–1197.

[22] Wekesa, D. W., Wang, C., Wei, Y., and Danao, L. A. M. (2014). Influence of operating conditions on unsteady wind performance of vertical axis wind turbines operating within a fluctuating free-stream: A numerical study. Journal of Wind Engineering and Industrial Aerodynamics, 135:76–89.

[23] Wilcox, D. C. (2008). Formulation of the k- ω turbulence model revisited. AIAA journal, 46(11):2823–2838.